CLM - P 94

CLM - P 94

United Kingdom Atomic Energy Authority

RESEARCH GROUP

Preprint

RADIAL DISTRIBUTION OF PLASMA FORMED IN SIMPLE MIRROR MACHINES BY FIELD IONIZATION OF FAST NEUTRAL ATOMS

E. G. MURPHY
A. C. RIVIERE
D. R. SWEETMAN

Culham Laboratory,

Culham, Abingdon, Berkshire

1966

UNCLASSIFIED
(Approved for Publication)

CLM – P 94

RADIAL DISTRIBUTION OF PLASMA FORMED IN SIMPLE MIRROR MACHINES BY FIELD IONIZATION OF FAST NEUTRAL ATOMS

by

E.G. MURPHY
A.C. RIVIERE
D.R. SWEETMAN

(Submitted for publication in Nuclear Fusion)

U.K.A.E.A. Research Group,
Culham Laboratory,
Nr. Abingdon,
Berks.

January, 1966

CONTENTS

		Page
1.	INTRODUCTION	1
2.	CALCULATION OF THE FRACTION IONIZED	1
3.	POPULATION OF THE EXCITED LEVELS IN THE ATOM BEAM	2
4.	DEPENDENCE OF FRACTION IONIZED ON FIELD GRADIENT COEFFICIENT α	4
5.	THE RADIAL DISTRIBUTION OF PLASMA	5
6.	EXPERIMENTAL OBSERVATIONS	6
7.	COMPARISON OF CALCULATED DISTRIBUTIONS WITH EXPERIMENT	9
8.	LIMITATION OF PLASMA SIZE BY PRE-IONIZATION	10
9.	CONCLUSION	10
	ACKNOWLEDGEMENT	11
	REFERENCES	11

A B S T R A C T

The radial distribution of plasma which results from field ionization of excited atoms injected into simple mirror machines is calculated and compared with measurements made in the PHOENIX machine. The excited atoms are assumed to have a level population distribution given by An^{-3} where n is the principal quantum number. The fraction of the atoms ionized per unit interval along their path is obtained by calculating the quantum mechanical barrier penetration probability at each point. Finite Larmor orbit diameter, precessional drift around the field axis and finite atom beam dimensions are taken into account in obtaining the radial distribution of plasma that results from this method of injection. The plasma distribution rises to a maximum on the axis in contrast to the distribution obtained by assuming ionization occurs immediately a critical field is reached. Good agreement with experiment is obtained both for the absolute density and for radial distributions.

The fraction ionized per unit interval is calculated for the ALICE and OGRA II experiments without their stabilising fields and it is found that this fraction is approximately proportional to the square root of the radial field gradient coefficient. However, the fraction ionized per unit interval is also calculated for an artifical flat-topped field shape and the results show that even in the absence of field gradient useful trapping can be obtained.

Calculations are also made of the effect of pre-ionization on the radial extent of the plasma.

1. INTRODUCTION

The trapping of excited atoms by field ionization has proved to be a useful method for injecting high energy protons into mirror machines [1]. In this paper the plasma distribution which results from this method of trapping is calculated for simple mirror machines, without multipole fields, and the calculations compared with experimental observations.

2. CALCULATION OF THE FRACTION IONIZED

We consider an atom moving with velocity v cm/sec in a direction perpendicular to a magnetic field of B gauss. In the coordinate frame in which the atom is at rest there is an electric field of strength 10^{-8} vB volt/cm and the electron finds itself in a field configuration with a potential barrier on one side. Ionization, and therefore trapping, will occur at the instant that the electron undergoes the quantum mechanical process of tunnelling through this barrier. The electron does not leave the atom immediately a critical value of field is reached but instead there is a finite probability for the tunnelling process to occur over a range of field strengths. We define this probability as $P(p,E)$ sec^{-1} where p represents all the quantum numbers which define the excited state and E is the field strength.

The method used to calculate $P(p,E)$ is similar to that of Lanczos [2] and was described by Bailey et al [3]. It is essentially a W.K.B. solution to the Schroedinger equation for a hydrogen atom in an electric field. It was shown by Hiskes [4] that for an atom moving in a magnetic field the equation for the internal motions is the same as in the electrostatic case but with E replaced by $\frac{vB}{c}$ and with the addition of the Zeeman energy term. The maximum Zeeman energy shift in a strong field in atomic units is given by [5].

$$\Delta W_z = \frac{B\, n\, \Upsilon}{2}$$

where n is the principal quantum number and Υ is the fine structure constant. The maximum Stark energy shift due to the electric field is

$$\Delta W_s = \frac{3}{2}\, n\, (n-1)\, vB\Upsilon.$$

The ratio of the energy shifts is therefore

$$\frac{\Delta W_S}{\Delta W_Z} = 3\ (n - 1)\ v$$

For a 20 keV hydrogen atom the velocity v in atomic units is 0.9 and in the mirror machines the lowest value of n (for which ionization occurs) is about 8 so that the Zeeman shift is at least one order of magnitude less than the Stark shift and is therefore neglected.

If the atoms in the beam are taken to be initially in one excited state p, and the beam has unit intensity, then the intensity $I(p,y')$ after travelling a distance y' in a field of strength $E(y) = 10^{-8}\ vB(y)$ is

$$I(p,y') = e^{-\int_o^{y'} P(p,E(y))\frac{dy}{v}} .$$

For simple mirror machines the dependence of the magnetic field strength B on the radius R in the median plane is given within the region of interest by $B = B_o\ (1 - \alpha R^2)$ where B_o is the field strength on the axis and the coefficient α is determined by the size and position of the coils. The values of α for three existing machines are PHOENIX: 0.0037 cm^{-2}, ALICE: 0.00063 cm^{-2} [6], and OGRA II: 0.000063 cm^{-2} [7]. The axial variation of field strength is only ± 4.5 per cent or less in the region of interest and will be neglected. We write the fraction ionized between y' and $y' + dy$ as

$$f(p,y') = -\frac{d}{dy}\ I(p,y') ,$$

so that if we consider a beam of atoms with a fraction $q(p)$ in each state p then the total fraction ionized in the interval dy is

$$F(y') = \sum_p f(p,y')\ \ q(p).$$

It is now necessary to determine the likely values of $q(p)$.

3. POPULATION OF THE EXCITED LEVELS IN THE ATOM BEAM

The beam of atoms with a proportion excited to high energy levels may be produced by dissociation of H_2^+ ions or by electron capture by protons in a gas cell. In injection experiments the gas target thickness is chosen so that several collisions occur. For electron capture in hydrogen gas the distribution amongst the

levels has been found to be approximately of the form An^{-3} [8]. Some more recent results [9] suggest that the distribution may be of the form $An^{-2.5}$ so that there is an uncertainty of 0.5 in the value of the exponent for n. The value -3 is used in this paper. The coefficient A depends on the particular gas used and the proton energy. At 20 keV it ranges for example from 0.24 for H_2 [8] to about 1.5 for Mg vapour [10]. The molecular vapour $C_8 F_{16}$ is used in the PHOENIX experiments. For this case a value of $A = 0.53$ was measured at $n = 11$ by the technique described by Riviere and Sweetman [8].

Since the field ionization probability depends on all quantum numbers, it is also necessary to consider the distribution amongst the substates. In the gas cell there is sufficient stray field present to ensure that the atoms in states with $n > 10$ will be in the linear Stark region. It was shown by Omidvar [11] that under these conditions the capture cross section is independent of the quantum numbers n_1, and n_2 so that the initial distribution amongst the substates will be uniform for a given value of m. Also there will be ions and electrons present due to ionization of the gas by the beam. Their density is estimated to be of the order of 10^{10} to 10^{11} cm^{-3} and the average cross section for scattering between the substates for $n = 10$ at 20 keV is approximately 10^{-10} cm^2 [12]. These collisions will ensure an essentially uniform statistical distribution amongst the substates as the atom beam leaves the gas cell.

Since the atom beam originates at some distance from the mirror machine (for PHOENIX this is 2.5 m, for ALICE 3.7 m [6] and for OGRA II 3.5 m [7]) some allowance must be made for radiative decay. As stated above the presence of stray fields means that Stark lifetimes must be used [13]. However the gas density and therefore the ion density is very much less than in the gas cell and it is estimated that the mean free path for collisional transfer from one sustate to another ranges from 10^2 to 10^5 cm. The mean free path for radiative decay averaged over the substates of the $n = 10$ level for a 20 keV atom is 60 cm. Radiative decay will therefore occur more rapidly than scattering between the substates and it is assumed in calculating decay that each substate behaves independently throughout the flight path.

4. DEPENDENCE OF FRACTION IONIZED ON FIELD GRADIENT COEFFICIENT α

The calculated fraction F(R) of a 30 keV atom beam which would be ionized in PHOENIX IA is shown in Fig.1 as a function of radius R for B_o = 25 kG. The upper graph shows the variation of magnetic field over the region considered. The group of curves in the lower graph shows the variation of the fraction ionized per cm for a few substates of the level n = 10. The upper curve is a sum of all substates of the levels which are ionized in the field range. For these results A = 1 and no correction was made for radiative decay.

The radial extent of the ionization of atoms in any given substate can be clearly seen as can its dependence on the field gradient. Also it can be seen that appreciable ionization occurs at the centre where the gradient is zero and also beyond the field maximum. These effects are a direct consequence of the quantum mechanical barrier penetration effect. On a classical basis the ionization would be zero at the axis and would not occur beyond the field maximum.

The peak in the composite curve is due to the level structure of the atom. As the field strength is decreased the peak moves towards the axis and gradually merges with the background. At no value of field strength does a peak in the composite curve actually appear on the axis.

TABLE 1

Fraction Ionized Per Centimetre Interval on Axis
for B_o= 10 kG and an Atom Energy of 20 keV

	$\alpha^{\frac{1}{2}}$ cm^{-1}	F(o) cm^{-1}
PHOENIX IA	0.061	1.57×10^{-5}
ALICE	0.025	6.87×10^{-6}
OGRA II	0.0079	2.18×10^{-6}

Values for the fraction ionized per centimetre path at zero radius for PHOENIX IA, ALICE and OGRA II are given in Table 1 together with the corresponding

values of $\alpha^{\frac{1}{2}}$. In each case the atom energy was taken to be 20 keV and B_o = 10 kG. The almost linear dependence of F(O) on $\alpha^{\frac{1}{2}}$ suggests that for $\alpha = 0$ no ionization will occur but this is only strictly true for a machine of correspondingly infinite diameter. In fact if the case of $\alpha = 0$ is taken but a finite size chosen for the field region then an appreciable fraction will be ionized within the region of interest. This is illustrated in Fig.2 where values of F(R) for a flat-topped field shape 50 cm wide and for OGRA II (the machine with the smallest α) are shown.

5. THE RADIAL DISTRIBUTION OF PLASMA

When a proton is trapped in a simple mirror machine it describes a nearly circular orbit with a radius given by $r_L = Mvc/eB$. Due to the radial gradient in B the guiding centre of this orbit precesses around the axis at a constant radius. The contribution to particle density is spread over an annulus whose width is defined by $2r_L$ and whose radius is related to the radius of the trapping point. The behaviour is illustrated in Fig.3. As pointed out in Section 2 the axial variation of magnetic field is small and is neglected so that the plasma distribution is calculated as a 'line density', that is, density integrated along a flux tube.

To obtain the radial distribution, a quantity C(X,Y,R) which takes into account the finite value of r_L is calculated at intervals in Y along each injection path of height X. C(X,Y,R) is the fractional contribution of protons formed at X,Y to the shell of radius R and is defined so that Σ_R C(X,Y,R) = 1. The total contribution to a shell of radius R is divided by the area of that shell to obtain the fractional contribution per unit area and thereby take into account the precessional drift around the axis. Finally the plasma distribution is given by

$$N(R) = \sum_X \sum_Y \frac{F(X,Y)\ C\ (X,Y,R)\ SHAPE\ (X)}{AREA\ (R)}$$

where F(X,Y) is the fraction ionized as calculated in section 2 for a path of

height X. The quantity SHAPE (X) is included to define the extent of the atom beam in the Z direction and its density profile and is defined so that Σ_x SHAPE (X) = 1. The quantity N(R) is in units of fraction of beam current per unit cross sectional area and the proton density can be obtained from this by multiplying by $J_o \cdot \tau$, where J_o is the total atom beam intensity and τ is the time constant for plasma decay.

Values of N(R) as a function of radius, for PHOENIX IA, are shown in Fig.4 as the curve labelled quantum effect field ionization. For these calculations B_o = 29.2 kG and the atom energy was 20 keV. Also shown in Fig.4 are values of N(R) based on a classical model for field ionization. In this case it is assumed that all atoms in a given state are ionized immediately their ionization probability exceeds 5×10^8 sec^{-1}. This probability is characteristic of the probabilities at which barrier penetration occurs in PHOENIX IA and is chosen merely to ensure that the same states are considered as in the quantum effect result. It can be seen that the proper treatment of barrier penetration effects leads to a much higher density on the axis than the 'immediate' ionization approximation. As can be seen in Fig.1 the radial extent of the ionization from one state becomes narrower as the field gradient increases and therefore at high field gradients the classical calculation will yield the same result as the quantum effect calculation. Values of N(R) for simple gas collisional ionization without field ionization are also shown in Fig.4. Here the assumption is made that a fixed fraction equal to 10^{-4} of the atom beam is ionized per cm of path. The effect of gas collisional ionization is to make the radial distribution more peaked at the centre than that of quantum effect field ionization.

6. EXPERIMENTAL OBSERVATIONS

In order to check the calculated radial distributions and absolute line densities experimental results were obtained for the plasma formed in the PHOENIX IA neutral injection machine by measuring the cold ion current flowing out along the field lines. In this experiment a beam of atoms with an energy of 20 keV is

produced by passing a 40 keV H_2^+ beam through a gas cell containing $C_8 F_{16}$. The beam is injected at right angles to the magnetic axis and protons and electrons are produced either by field ionization or by collisions with background gas molecules. In the absence of instabilities or scattering the fast protons are trapped in the magnetic field until charge exchange with the background gas enables them to escape. It can be shown that each fast proton produces $1 + \sigma_i/\sigma_x$ slow ions, where σ_i is the cross section for production of electrons and σ_x is that for charge exchange. The background gas in the experiment was helium for which the above ratio is 1.2. Values of the cross sections were taken from Gilbody and Hasted [14] for σ_i and Stier and Barnett [15] for σ_x.

The cold ions and electrons in the plasma can only escape along the field lines and this fact can be used to measure the radial distribution of fast ions from outside the plasma region. If the slow ion component is measured the fractional line density as defined in Section 5 can be obtained by the relation

$$N(R) = \frac{2\, I(R_c)}{J_o} \; \frac{1}{1 + \sigma_i/\sigma_x} \; \frac{1}{S\, B(R_c)/B(R)}$$

where $I(R_c)$ is the cold ion current through one mirror at the radius R_c

J_o is the total atom beam current

S is the area of the current collector

$B(R_c)$ is the magnetic field at the collector and

$B(R)$ is the magnetic field at the midplane on the same field line as the collector.

The factor 2 arises because half of the total ion current has been shown to leave through each mirror coil.

The slow ion currents were measured at various radii by a system of collectors 1 × 0.4 cm in area placed in the throat of the mirror region. A schematic diagram of the electrode system is shown in Fig.5. The first electrode was connected to earth. With a positive potential applied to the second electrode to repel all ions, a potential of -25 volt on the third electrode was found to be sufficient to repel all electrons; this potential was considered to be sufficient to suppress

secondary emission from the collector. Normally the second electrode was connected to earth; under these conditions the ion current decreased by 20 per cent when the potential on the third electrode was changed to -100 volt. This was thought to be due to the defocussing effect of the component of the electric field perpendicular to the magnetic field near the sides of the slot. The effect disappeared when the central collector was rotated through 90^{o} and thus did not collect ions which passed close to the electrodes. Absolute measurements of slow ion current were taken with the central collector in this position but it was not possible to do this for all radii and therefore the radial distributions were measured with all collectors in the positions shown in Fig.5 and normalised to the absolute value at the centre. The cold ion currents were of the order of 10^{-9} amp and were measured as voltages across 10 MΩ using cathode followers with input time constants of about 200 μsec.

In order to ensure a stable plasma for the measurements, it was necessary to lower the plasma density. This was achieved by raising the background gas pressure to the point where the charge exchange time constant was equal to 2.5 $\pm$ 0.5 msec. It was essential that the plasma potential should be positive in order to drive the cold ions out through the mirrors in a short time. The plasma potential was established to be about + 10 V for these measurements. At the gas pressure used the ionization of the atom beam by gas collisions gave a contribution to N(R) of $1.0 \pm 0.3 \times 10^{-7}$ cm^{-2} at zero radius. The error due to ionization of the background gas by electrons was negligible. The experimental results were not corrected for these effects.

The magnetic field was pulsed, rising to a maximum of 50 kG in about 1 sec and then decaying with a time constant of about 1 sec. The maximum rate of rise where readings were taken was about 1 per cent per millisecond. This was slightly greater than the ideal but the error introduced is estimated to be less than 10 per cent and would have the effect of smoothing out the variation of the quantity N(R) with magnetic field strength.

The injected atom beam with an intensity of about 8 mA equivalent was monitored by measuring the secondary emission from a water cooled metal plate on which the beam impinged after passing through the magnetic field. This in turn was calibrated by using the same plate as a calorimeter.

7. COMPARISON OF CALCULATED DISTRIBUTIONS WITH EXPERIMENT

Values of N(R) at $R = 0$ for PHOENIX IA are shown in Fig.6 as a function of magnetic field strength. The dashed and dot-dashed curves are the calculated values with and without correction for radiative decay respectively. The series of peaks in the curve show the variation in N(R) as each successive quantum level in turn makes the principal contribution to the plasma. Parameters appropriate to the experimental conditions (circular atom beam of diameter 4.5 cm and an atom energy of 20 keV) were used to enable a direct comparison with the experimental results which are shown in Fig.6 as the solid curve. The agreement is better than either the error in measuring A for $C_8 F_{16}$ which was ± 20 per cent or the absolute error in the PHOENIX IA measurements which was ± 25 per cent at low field strengths and ± 20 per cent at high field strengths. The results suggest that $An^{-2.5}$ may be a better assumption for the initial distribution than An^{-3}; the calculated curve would pivot about $n = 11$ since the value of A was measured at this point.

The calculated and measured value of N(R) as a function of radius are shown in Fig.7 for eight magnetic field values from 10.8 to 44.6 kG. The experimental points have been normalised to fit the curve near the centre. For these measurements the plasma radius was limited to 10 cm by a metal plate and the dashed lines represent the assumption that the density falls linearly to zero at the limiter in one Larmor diameter. The length of the arrow in each case represents the diameter of the proton orbit which just touches the limiter. The experimental results are in good agreement with the quantum mechanical calculations and it is evident (c. f. Fig.4) that the classical model for field ionization gives the wrong result.

8. LIMITATION OF PLASMA SIZE BY PRE-IONIZATION

It is possible that instead of using a mechanical plasma limiter the same effect could be achieved by using a pre-ionizing field in the flight path of the atom beam since the plasma appearing at a given radius is related to a particular excited level. To calculate this possibility a pre-ionizing magnetic field shape of the form

$$B = B_{max}(1 - a\,x^2 + b\,x^4)$$

where $a = 5.69 \times 10^{-3}\ cm^{-2}$ and $b = 8.58 \times 10^{-6}\ cm^{-4}$ was used since this corresponds to that found for an existing electromagnet. The loss of population of a given substate is simply

$$e^{-\quad P(p,E(x))\ \frac{dx}{v}}.$$

Values of N(R) for PHOENIX IA with $B_o = 20$ kG and an atom energy of 20 keV are shown in Fig.8 for pre-ionizing field strengths $B_{max} = 0$, 15 and 17 kG. It can be seen that the plasma is limited in a similar manner to that achieved by a mechanical limiter but leaves the possibility of controlling the radial density gradient at the edge of the plasma. The assumption that the substates retained their identity between pre-ionizing field and mirror machine was made, but if it is assumed that the population of all substates of a given level are redistributed statistically then approximately the same limitation in radius is obtained but there is a small overall loss in plasma density.

9. CONCLUSION

The inclusion of the quantum mechanical effect leads to higher densities on the magnetic field axis than are predicted by the simple classical model. This is a consequence of the fact that the barrier penetration effect produces ionization where the field gradient is zero and also beyond the magnetic field maximum. The agreement between the predicted and measured radial distributions indicate the essential correctness of the quantum mechanical treatment. For large enough field gradients, however, it is expected that the classical approach would be satisfactory.

The experimental results show that the population of excited levels in the atom beam falls off more slowly than An^{-3} and that $An^{-2.5}$ may be a better assumption.

Also, a pre-ionizing magnetic field may be used to limit the radial enter of the plasma and possibly to control the radial density gradient at the edge of the plasma.

ACKNOWLEDGEMENT

The authors thank A.I. Kilvington, I.I. King and the PHOENIX operating team for their valuable assistance.

REFERENCES

1. BERNSTEIN W., et al. Paper No.21/232, Proc. IAEA Conf. on Plasma Physics and controlled Nuclear Fusion Research, Culham, U.K., Sept. (1965); A.H. Futch, Jr. et al. Paper No. 21/234, loc. cit; L.I. Artemenkov et al. Paper No. 21/238, loc. cit.
2. LANCZOS, C. Z. Physik 68 (1931) 204.
3. BAILEY D.S., HISKES, J.R. and RIVIERE, A.C. Nuclear Fusion 5 (1965) 41.
4. HISKES, J.R. Nuclear Fusion 2 (1962) 38-48.
5. See for example: BETHE, H.A. and SALPETER, E.E. Quantum Mechanics of One and Two Electron Atoms, Springer-Verlag, Berlin (1957) p.205.
6. Private communication.
7. Private communication.
8. RIVIERE, A.C. and SWEETMAN, D.R. Proc. Third Int. Conf. Physics of Electronic and Atomic Collisions, London, 1963, North Holland Publishing Co., Amsterdam (1964), p.734.
9. BOBASHEV, S.V., ANKUDINOV, V.A. and ANDREEV, E.P. Soviet Physics J.E.T.P., 21 (1965) 554-556.
10. ILIN, R.N., OPARIN, V.A., SOLOVYOV, E.S. and FEDORENKO, N.V. Presented at Fourth Int. Conf. Physics of Electronic and Atomic Collisions, Quebec, 1965.
11. OMIDVAR, K. Unpublished report no. X-641-65-306, Goddard Space Flight Center, Greenbelt, Maryland, U.S.A. (1965).
12. MAY, R.M. and BUTLER, S.T. Phys. Rev. 138 (1965) 1586-1591.
13. HISKES, J.R., TARTER, C.B. and MOODY, D.A. Phys. Rev. 133 (1964), 424-426.
14. GILBODY, H.B. and HASTED, J.B. Proc. Roy. Soc., A240 (1957) 382-395.
15. STIER, P.M. and BARNETT, C.F. Phys. Rev. 103 (1956) 896-907.

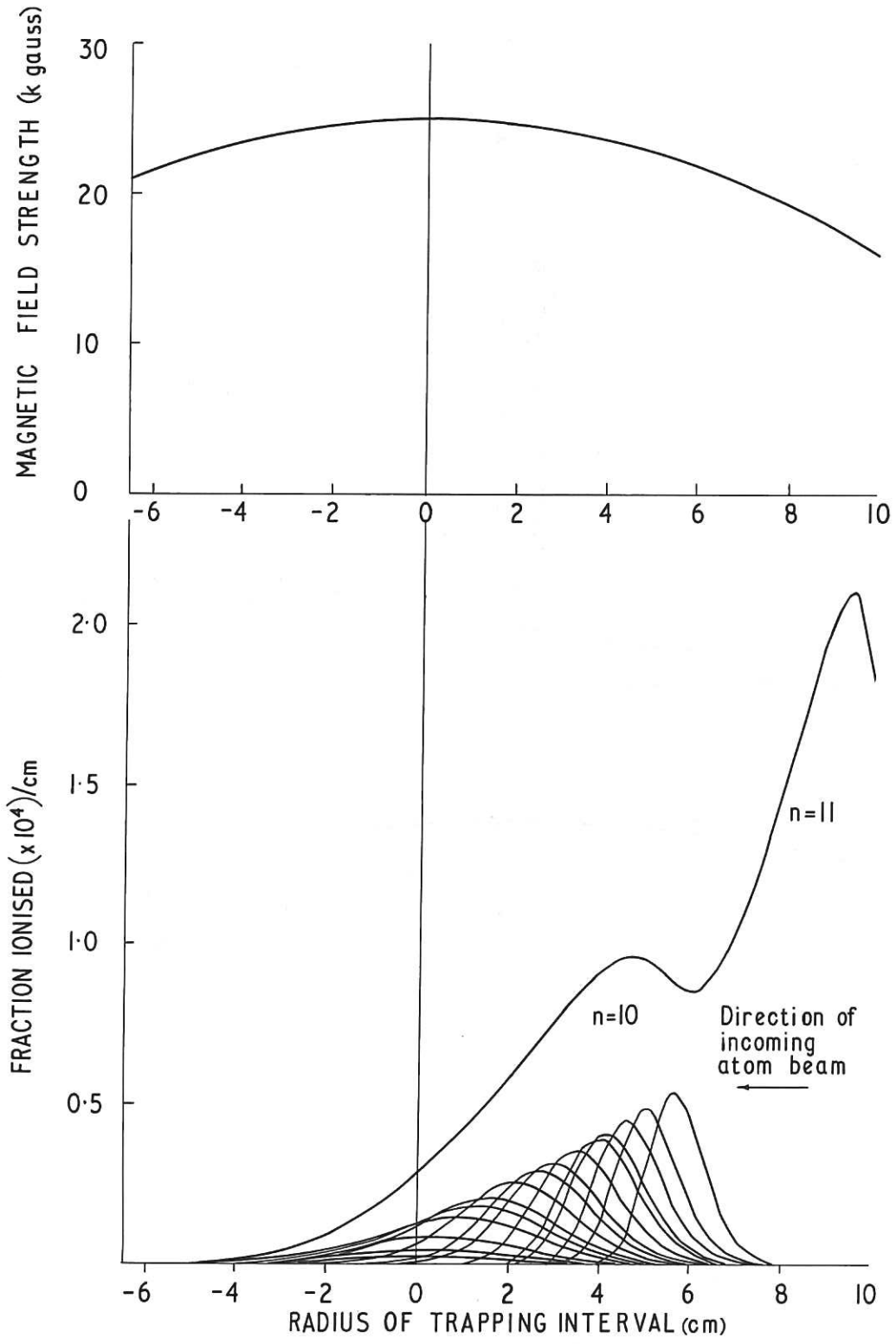

Fig.1 CLM-P94

Upper Curve: magnetic field strength in median plane as a function of radius. Lower Curves: fraction of atom beam ionized per centimeter interval as a function of radius. Curves are shown for some individual substates of the level n = 10 and a composite curve is shown which is a statistical sum of all the substates of n = 10, 11 and 12.

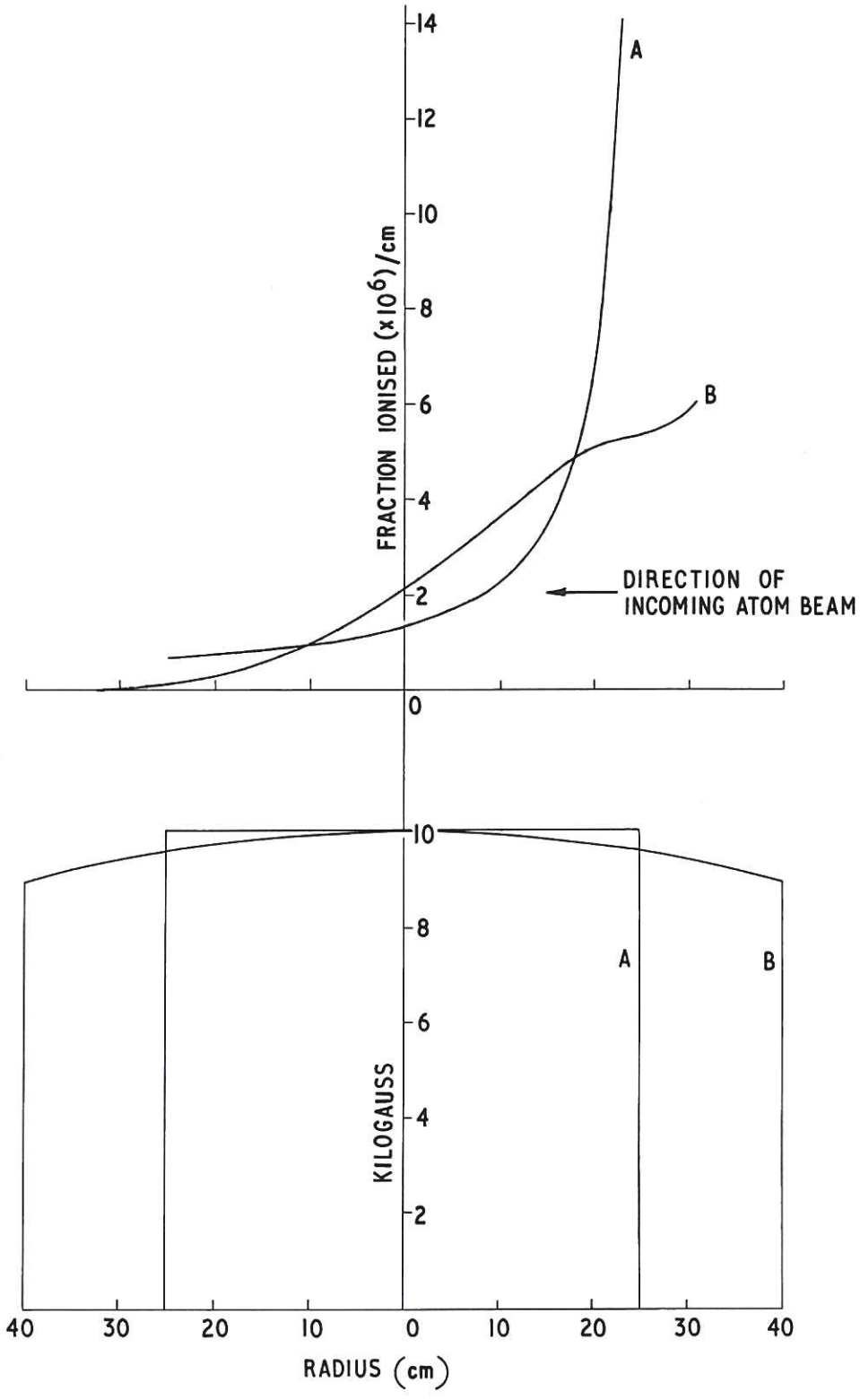

Fig.2 CLM-P94

Lower Curves: magnetic field strength in median plane as a function of radius for (a) artifical flat topped field shape and (b) the OGRA II field shape. Upper Curves: fraction of atom beam ionized per centimetre interval as a function of radius for magnetic field shapes (a) and (b) of lower curves respectively.

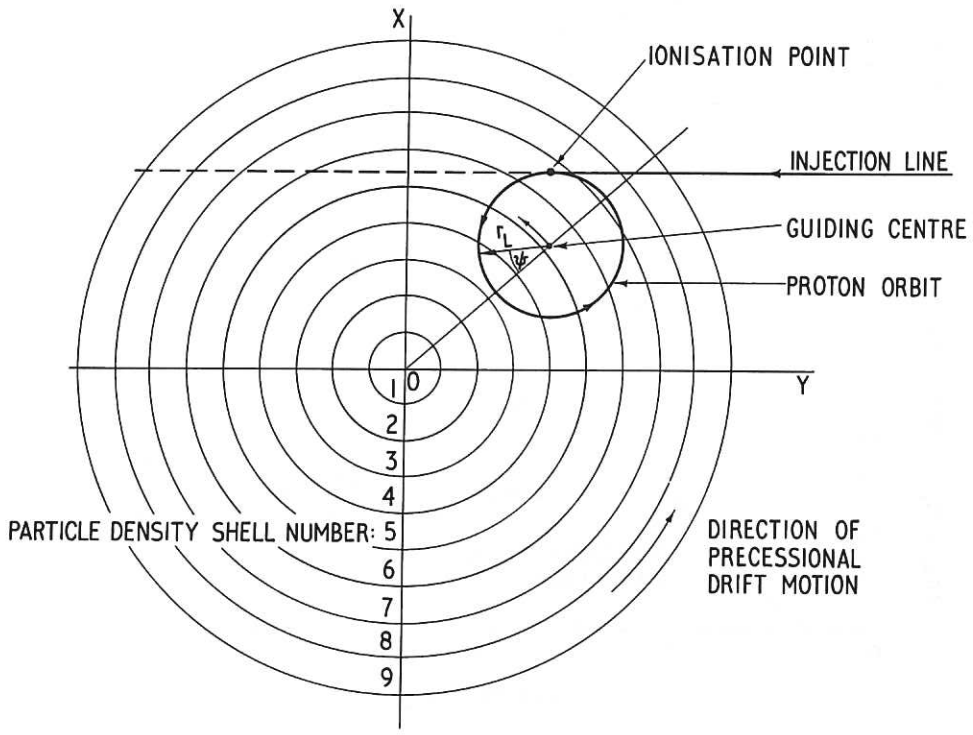

Fig.3 CLM--P 94

Illustration to show contribution which one proton makes to radial distribution allowing for finite Larmor orbit diameter, precessional drift around field axis and finite atom beam size in the X direction.

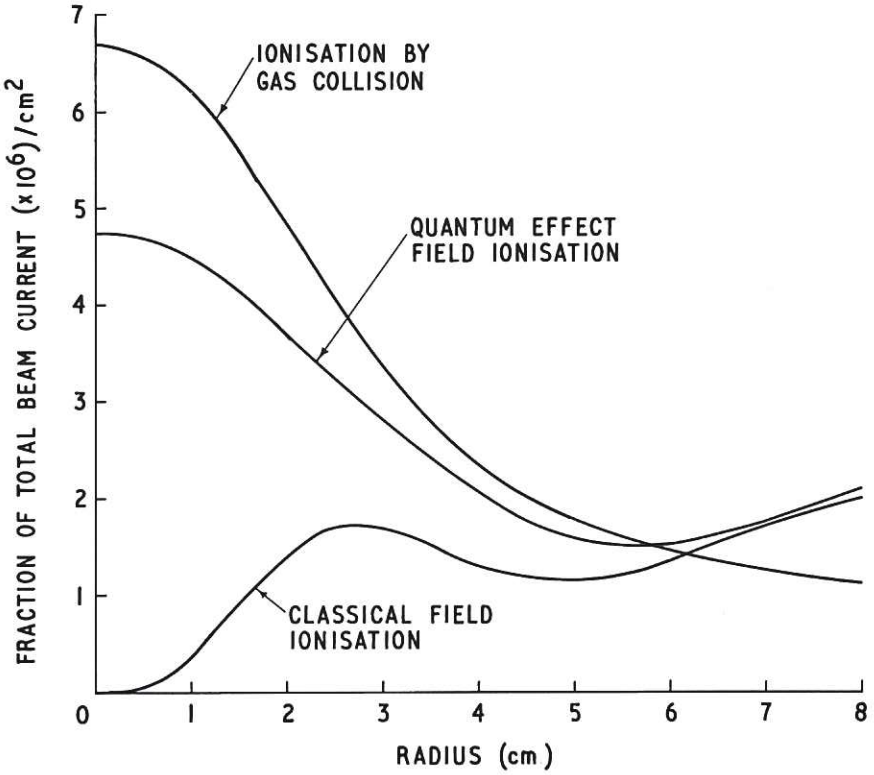

Fig.4 CLM-P94

Radial distribution of plasma arising from quantum effect field ionization, classical field ionization and gas collisions for an atom energy of 20 keV and central field of 29.2 kG

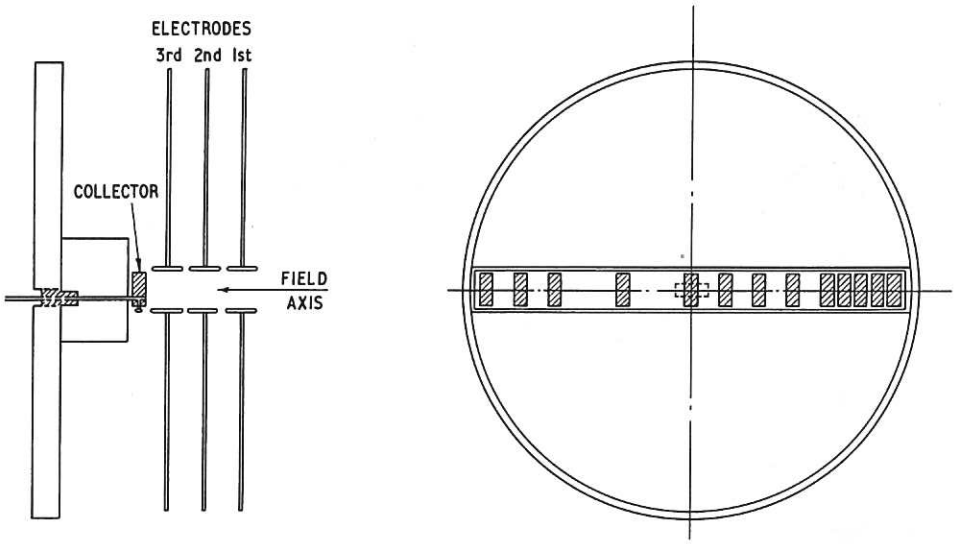

Fig.5 CLM-P94

Schematic diagram of collector electrode system used to measure radial distribution of slow ion currents flowing out of plasma along the field lines.

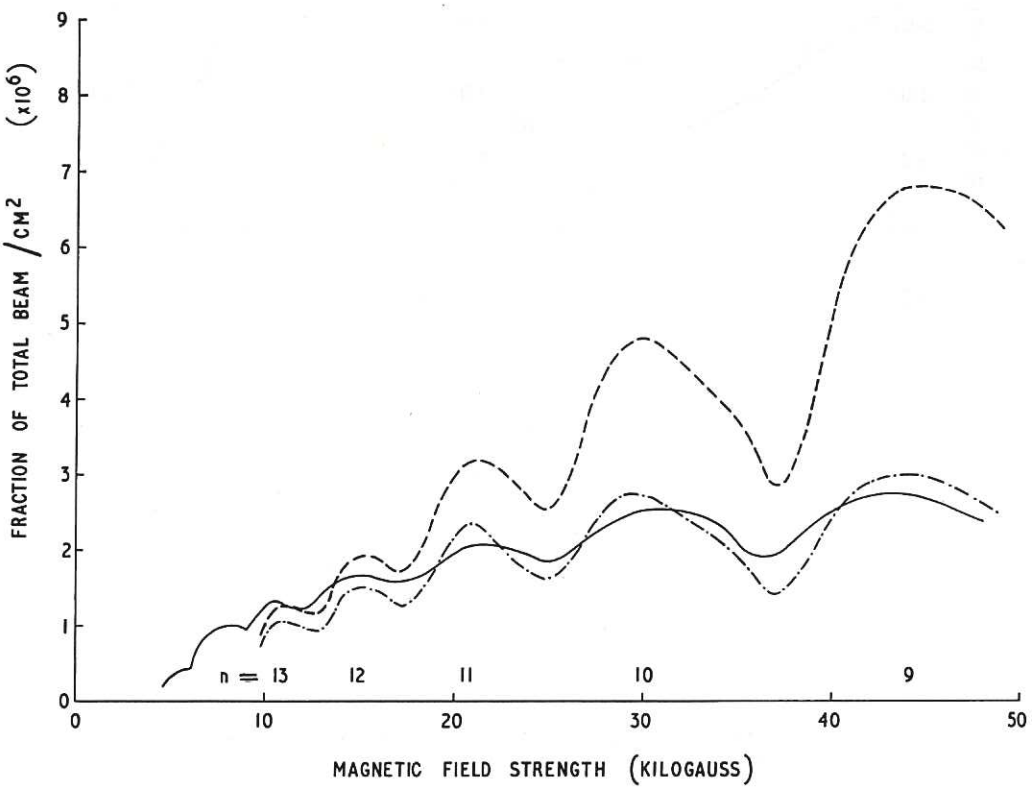

Fig.6 CLM-P94

Fractional line density on the axis for PHOENIX IA as a function of magnetic field strength for an atom energy of 20 keV. The population of the levels is given by $0.53\ n^{-3}$ for the dashed curve. Decay over a flight path of 2.5 metres is included in the dot-dashed curve. Experimental values are shown as the solid curve and have a possible systematic error of 25% at 10 kG and 20% at 45 kG.

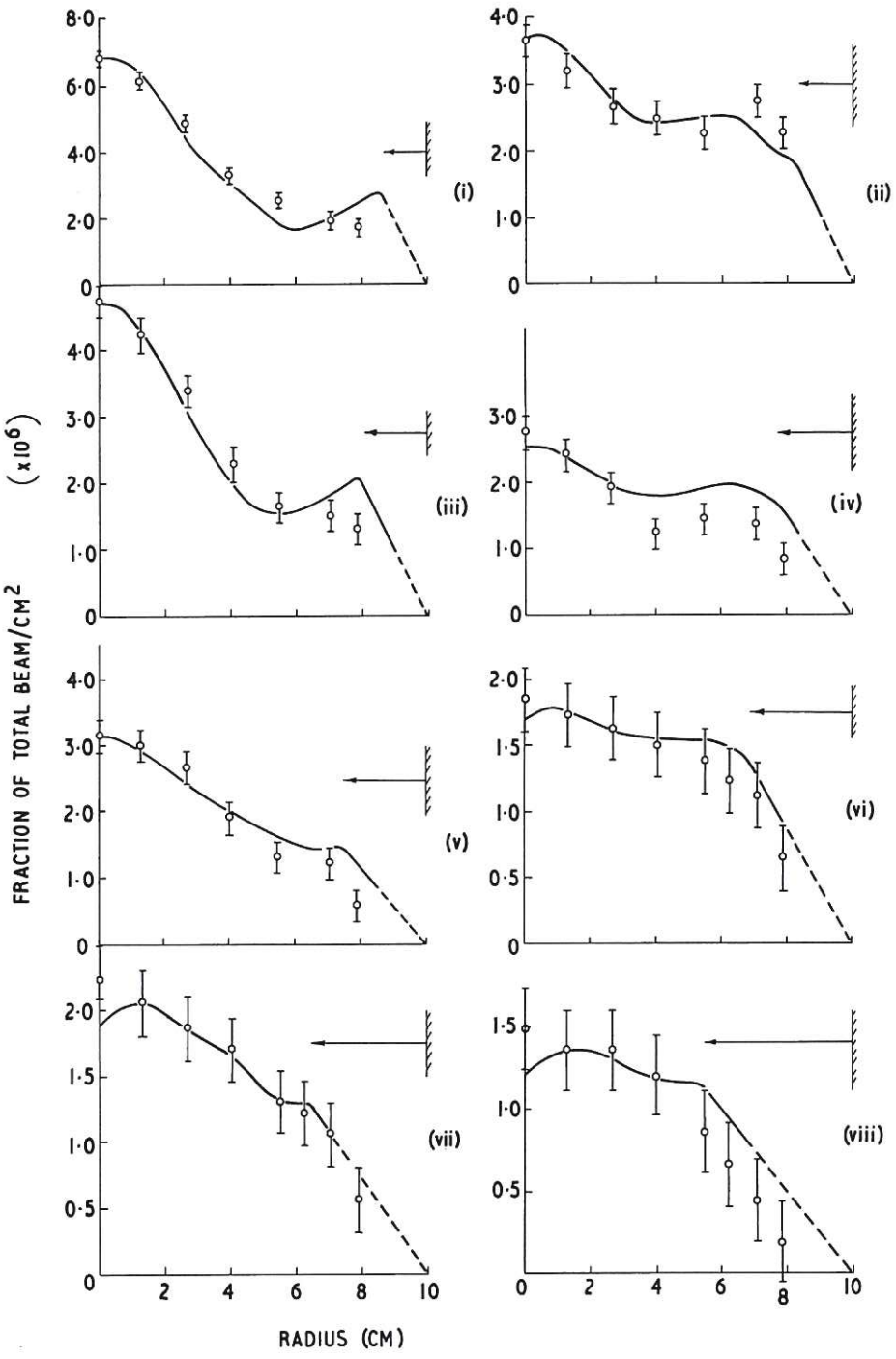

Fig.7 CLM-P94

Radial distribution of plasma for PHOENIX IA as a function of radius for an atom energy of 20 keV. The magnetic field strengths on axis in kG are: (i) 44.6: (ii) 35.0: (iii) 29.2: (iv) 25.0: (v) 22.0: (vi) 17.3: (vii) 15.5: (viii) 10.8. Solid curves are calculated distributions and open circles are experimental results. The shaded lines indicate the location of the plasma limiter and the length of the arrows is equal to the diameter of the proton orbits which touch the limiter.

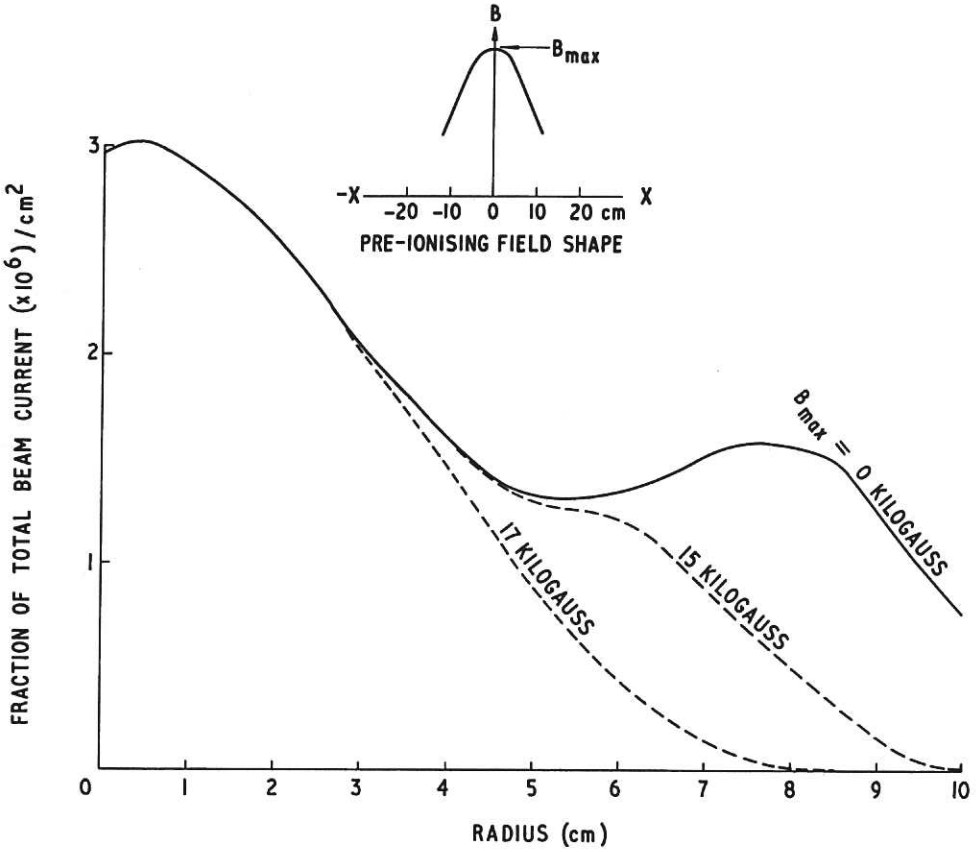

Fig.8 CLM-P94

Calculated radial distribution of plasma for PHOENIX IA as a function of radius for an atom energy of 20 keV and central field of 20 kG. Results are shown for pre-ionizing field strengths of 0, 15 and 17 kG